Macromolecules

Article

Cite This: Macromolecules 2017, 50, 8097-8105

pubs.acs.org/Macromolecules

Thermal Control of Confined Crystallization within P3EHT Block Copolymer Microdomains

Emily C. Davidson[†] and Rachel A. Segalman*[,†,‡]

[†]Department of Chemical Engineering and [‡]Materials Department, University of California, Santa Barbara, Santa Barbara, California 93106, United States

Supporting Information

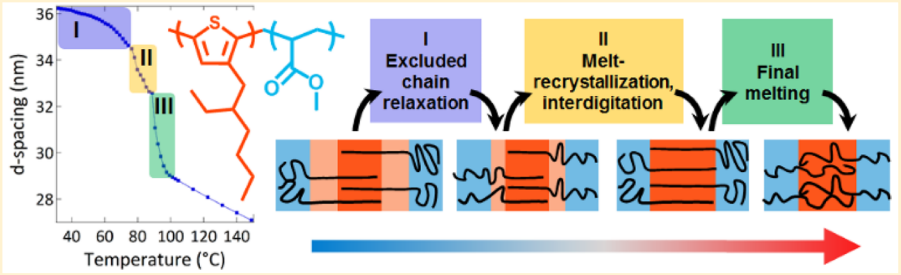

ABSTRACT: The local, nanoscale organization of crystallites in conjugated polymers is often critical to determining the charge transport properties of the system. Block copolymer geometries, which offer controlled nanostructures with tethering of chains at interfaces, are an ideal platform to study the local organization of conjugated polymer crystallites. The model conjugated polymer poly(3-(2′-ethyl)hexylthiophene) (P3EHT) features a depressed melting temperature relative to the widely studied poly(3-hexylthiophene) (P3HT), which allows it to robustly form microphase-separated domains that confine the subsequent P3EHT crystallites. Importantly, P3EHT crystallization in confinement is coupled to a rubbery second block via interfacial tethering, mechanical properties, and chain stretching. Here, the impact of thermal processing on the diblock copolymer structure is examined to elucidate the key driving forces controlling the final coupled diblock copolymer and crystalline structures. Surprisingly, the diblock copolymer domain size is significantly impacted by the temperature at which the conjugated domain is crystallized. Decreasing amounts of domain extension are observed with increasing crystallization temperatures. This temperature-dependent domain structure appears to be correlated with the crystallization processes; these processes are inferred from precise changes in the lamellar structure across melting. By carefully tracking the changes in domain structure across melting, this work identifies three distinct regimes. We suggest a structural model of the conjugated block melting processes consisting of (I) excluded-chain relaxation, followed by (II) chain interdigitation during melt-recrystallization, and finally (III) complete melting that is independent of the initial crystallization conditions. These results suggest that P3EHT crystallization processes associated with temperature-dependent chain diffusion and nucleation are primarily responsible for the unexpected temperature-dependent crystallization behavior. They also emphasize that less perfect conjugated polymer crystals may actually be associated with a poorly interdigitated structure. Furthermore, this work demonstrates the utility of leveraging a diblock copolymer structure with a rubbery second block in order to precisely track changes in the crystallite structure.

INTRODUCTION

Conjugated polymers have been utilized in applications including photovoltaics, light-emitting diodes, and field effect transistors.[1−3] Importantly, the performance of these devices depends upon the charge transport properties of the constituent polymer, which in turn varies with the material's crystallinity.[4−11] Block copolymers containing crystalline conjugated blocks are of interest for incorporating both nanopatterning and conjugated polymers into a single material; furthermore, confinement of conjugated polymers within block copolymer microdomains provides an opportunity to study conjugated polymer crystallization in highly defined geometries with tethered chains at the boundaries. These structures are a versatile platform for crystallization studies; diblock copolymers allow variable control over molecular weight, interfacial curvature, interfacial area, and coupled chain dynamics to elucidate the relative forces driving and controlling the polymer crystallization. Thermal processing conditions exert considerable influence on both traditional and conjugated polymer crystallites, both in homopolymers and in confinement; further, the amorphous block of crystalline−amorphous block copolymers can have considerable influence over the dynamics, orientation, and folding of the crystalline material. This work focuses on understanding the interplay between thermal processing, chain dynamics, and polymer diffusion and

Received: July 27, 2017
Revised: October 3, 2017
Published: October 13, 2017

DOI: 10.1021/acs.macromol.7b01616
Macromolecules 2017, 50, 8097−8105

nucleation processes of a conjugated polymer crystallized in lamellar confinement.

Achieving controlled confined crystallization of conjugated polymers within block copolymer microdomains requires a system that meets several basic criteria and also achieves a critical balance of relevant forces. First, it is essential that the diblock copolymer system has a T_{ODT} greater than the melting temperature of the component conjugated polymer.[12,13] Meeting this criteria alone is challenging given that conjugated polymers generally have extremely high melting temperatures (in excess of 200 °C). These high melting temperatures make it challenging to access microphase-separated melts from which confined crystallites can develop. Because of these high melting temperatures, many attempts at incorporating conjugated polymers within microphase-separated diblock copolymers have resulted in crystallization-driven self-assembly.[14,15] Even in those cases where a microphase-separated melt is accessible, the driving force for crystallization may still be large enough relative to the forces maintaining microphase separation to result in breakout crystallization, destroying the microdomain structure. These criteria in a conjugated polymer containing system may be satisfied by leveraging a poly(3-alkylthiophene) with a modified side-chain, poly(3-(2′-ethyl)hexylthiophene) (P3EHT). The modified side-chain depresses the melting temperature to only ∼80 °C, permitting the robust formation of microphase-separated P3EHT microdomains which may subsequently crystallize.[16,17]

Beyond simply achieving confined crystallization, identifying the relative driving forces that contribute to the final domain and crystalline structure is important for developing a deeper understanding of conjugated polymer crystallinity and for identifying critical design and processing parameters controlling these hierarchical block copolymers. Conventional polymers such as polyethylene develop chain-folded lamellae[18] where a single chain may span many lamellae when crystallized from the melt, resulting in a crystalline chain conformation that is minimally disturbed from its melt conformation. By contrast, an important driving force with a conjugated crystallizable block is the relatively strong preference for extended-chain crystallization in P3ATs; particularly at moderate molecular weights, regioregular (defect-free) poly(3-alkylthiophene) (P3AT) homopolymers are observed to form extended chain crystals at molecular weights of up to ∼10k.[19] These extended chain crystallites are driven by the relative stiffness of P3AT chains combined with the drive to maintain conjugation. While P3ATs have a persistence length in solution and in the melt of ∼3 nm[20] (significantly larger than hydrogenated polynorbornenes[21] that demonstrate chain folding at much lower molecular weights[22]), it is important to realize that P3AT flexibility arises from two local monomer−monomer conformations (syn vs anti) that can accommodate conjugation.[20] Crystalline packing, however, is only accommodated by the anti conformation,[5] and neither the local syn nor the anti conformation accommodates the sharp local turn required for chain folding (particularly in confinement) without significant conjugation-breaking bond torsion, thus favoring extended chain crystallites. At higher molecular weights, P3ATs in homopolymers begin to form tie-chains spanning multiple individual crystallites, which are important for allowing charge transport between individual crystallites.[9,23−25]

Prior work on lamellar P3EHT-*b*-PMA found that this preference for adopting an extended chain configuration places constraints on the conditions required for confined crystallization. In particular, the stiff nature of the P3EHT chains during crystallization induces the orientation of the resulting crystallites such that chains orient perpendicular to the microdomain interface. Furthermore, achieving fully extended crystals with this orientation appears to be essential to crystallization; the diblock copolymers with P3EHT confined in a glassy polystyrene (PS) matrix microphase separate but suppress crystallization.[26] The morphology and perfection of conjugated crystallites are highly impacted by thermal history; therefore, modifying the thermal processing of the diblock copolymer is expected to moderate the driving forces controlling the final crystalline and domain structure of the conjugated-*b*-amorphous polymer. Work on both P3EHT homopolymer and on P3EHT-*b*-PMA found that P3EHT crystalline perfection can be manipulated through the system's isothermal crystallization temperature; decreasing the degree of undercooling resulted in more highly perfect crystallites.[26,27] Further, while P3EHT in cylindrical confinement displays a change in nucleation mechanism that prevents crystallization at high T_c, it was demonstrated that an imperfect crystallite population initially formed at a large undercooling could be annealed at just below the melting temperature to form a single, highly perfect crystallite population.[28] Conventional wisdom attributes this increased perfection to changes in ordering along the monomer−monomer (chain) direction, where improvements in crystallinity directly correspond to improved chain extension.[29−31] Comparisons to P3EHT homopolymer led to the conclusion that in both P3EHT homopolymer and lamellar diblock copolymers, these improvements in crystallinity instead corresponded primarily to improvements in order along the π-stacking order direction.[26,27] Therefore, it is expected that improvements in confined P3EHT crystallite quality will not affect the overall domain spacing if changes in crystalline perfection are truly restricted to the π-stacking order direction; otherwise, domains are expected to be larger with increasing crystallization temperature if crystallite perfection is associated with improved P3EHT monomer−monomer ordering.

Importantly, the bias of conjugated polymers toward forming extended-chain crystallites is not the only factor expected to influence the self-assembly and crystallinity of conjugated-*b*-amorphous materials. The kinetics of the crystallization process itself are also highly temperature dependent. At small degrees of undercooling, chain diffusion processes are typically fast relative to nucleation processes, causing crystallization to be nucleation limited; at lower temperatures, crystallites may readily form stable nuclei, but crystallization may be limited by the time scales required for chains to diffuse and add to growing crystallites. Diffusion versus nucleation limited regimes are expected to induce distinct features on crystallite morphology and chain organization. Recent isothermal crystallization kinetics studies of P3EHT homopolymer indicates that the transition from diffusion limited to nucleation limited regimes occurs at T_c = ∼60 °C (the transition is, as expected, molecular weight dependent).[32] Understanding the impact of thermal processing conditions over these limiting regimes is expected to have significant impact on controlling the final crystalline and domain structure. It is important to note that in confinement the transition from diffusion to nucleation limited regimes is expected to shift to higher temperatures given that interfacial chain tethering limits chain diffusion.

Furthermore, the amorphous block is expected to intrinsically play a significant role in the resulting diblock copolymer

DOI: 10.1021/acs.macromol.7b01616
Macromolecules 2017, 50, 8097−8105

structure. As P3EHT forms extended-chain crystallites and the P3EHT microdomain extends laterally, the PMA domain is forced to also expand due to conservation of volume, stretching the PMA chains. Essentially, the conformation of the crystalline polymer directly impacts the effective area per chain at the diblock copolymer interface, which in turn modulates the degree of chain stretching induced in the amorphous block.[33,34] Importantly, theory predicts that a fold in the P3EHT chains forming the crystallites is capable of relieving this penalty. Furthermore, crystallite reorientation as a function of temperature in some flexible crystalline-*b*-amorphous systems has also been observed and hypothesized to be due to moderation of amorphous block stretching. In other studies of high-crystallinity hydrogenated polynorbornene containing diblocks, the number of folds in the crystallites was directly moderated by varying the length of the amorphous block; the amorphous block is believed to actually induce an equilibrium degree of chain folding in the crystalline block.[22] Thus, it is expected that the amorphous block stretching penalty is potentially a significant temperature-sensitive structural driving force in this system.[35,36]

Interestingly, other systems of conjugated polymers have displayed surprising changes in domain structure with temperature, suggesting that there are some universal processes in the structure formation and resolution in these materials that are still not well-understood. For example, the model rod−coil system DEH-PPV-*b*-PI displays a show shrinkage with increasing temperature that cannot be easily attributed to a change in liquid crystalline phase or other packing considerations. PPV is sufficiently stiff to fully inhibit chain folding at the molecular weights used in this study, indicating that other mechanisms—perhaps present in conjugated diblock copolymers—are driving these structural transitions.[37]

This work studies the response of P3EHT-*b*-PMA self-assembly and crystallization to changing thermal processing conditions in order to identify the key forces controlling the final domain and crystalline structure. The amorphous block deformability is critical to achieving P3EHT crystallization; importantly for this study, it also allows changes in the domain structure of the diblock copolymer as a whole to reflect chain reorganization in the P3EHT block. Here, the P3EHT-*b*-PMA domain structure is examined both as a function of isothermal crystallization temperature and across the melting process to investigate the interplay between crystallization and domain structure. P3EHT-*b*-PMA domains expand the most at the lowest crystallization temperatures, contradictory to our expectations that the more perfect crystallites formed at high temperatures correspond to the most extended chain crystallites. We examine several possibilities for this behavior and suggest a driving mechanism associated with crystallites featuring excluded crystallization and poorly interdigitated chains developing at low crystallization temperatures. Furthermore, this work both provides unique insight into the processes of achieving improved crystalline perfection in conjugated polymers as well as demonstrates the utility of block copolymer architectures to access unique features of conjugated polymer crystallization that would be difficult to access via other means.

EXPERIMENTAL SECTION

Synthesis. Reagents and solvents were used as received from Sigma-Aldrich. P3EHT monomer was synthesized as previously described.[16] P3EHT and PMA were synthesized via ethynyl-terminated GRIM and ATRP followed by azide substitution, respectively.[16,26] P3EHT-*b*-PMA was synthesized via coupling of component blocks by azide−alkyne click chemistry as previously described.[26] P3EHT and PMA without end-functionalization were synthesized via acid-terminated GRIM and by ATRP without an azide substitution, respectively. Preparation of blends is discussed in the Supporting Information.

Molecular Characterization. Gel permeation chromatography (GPC) to determine molecular weights and dispersity relative to PS standards was performed on a Waters instrument using Agilent PLgel 5 μm MiniMIX-D columns. The mobile phase was THF at 35 °C with a flow rate of 0.3 mL/min. ^{1}H NMR spectra were collected on a Varian VNMRS 600 MHz spectrometer using deuterated chloroform (Cambridge) as the solvent with ∼1 wt % polymer. Reported molecular weights are by end-group analysis. Volume fractions are calculated using densities from gas pycnometry and literature as previously described.[26] Molecular characterization of P3EHT-*b*-PMA 11.1K/6.0K is previously reported.[26] H-terminated P3EHT homopolymer has a dispersity of 1.15 and a molecular weight of 11.3k by ^{1}H NMR. PMA homopolymer has a dispersity of 1.13 and molecular weight of 5.0k by ^{1}H NMR.

Table 1. Molecular Characteristics of Polymers Used in This Study

polymer	dispersity ($Đ$)	^{1}H NMR mol wt
P3EHT-*b*-PMA	1.14	11.1k/6.0k
P3EHT-*b*-PMA	1.15	11.1k/8.0k
P3EHT-*b*-PMA	1.17	9.7k/9.5k
P3EHT-*b*-PMA	1.20	8.3k/9.8k
P3EHT-*b*-PMA	1.15	8.3k/8.8k
P3EHT	1.15	11.3k
PMA	1.13	5.0k

Differential Scanning Calorimetry. Samples for DSC were prepared by hermetically sealing between 1 and 10 mg of material inside TZero aluminum pans. Thermal processing is performed offline due to the long time scales associated with crystallization. Before each experiment, samples are heated to 150 °C offline and held for 10 min to clear thermal history. Isothermal crystallization of each blend was performed for 1 week in temperature-controlled ovens. Annealed samples are first crystallized at room temperature for a week and then annealed in temperature-controlled ovens overnight. DSC traces on heating were collected on a TA Q2000 calorimeter by heating from −20 to 150 °C at 10 °C/min.

Small- and Wide-Angle X-ray Scattering. Isotropic samples for X-ray scattering were prepared by melt-pressing into 1 mm thick aluminum washers at 150 °C. Samples were isothermally crystallized for 1 week within temperature-controlled ovens prior to data collection. Annealed samples were first crystallized at room temperature for 1 week and then annealed in temperature-controlled ovens overnight. X-ray scattering collected upon melting was performed on a controlled heat stage at beamline 7.3.3 at the Advanced Light Source; data were collected with 2 °C temperature resolution, and a 5 min wait time was used to allow the temperature of each sample to stabilize and equilibrate. SAXS 2-D patterns were collected at the Advanced Light Source (ALS) beamline 7.3.3 and at the Stanford Synchrotron Radiation Lightsource (SSRL) beamline 1-5. Silver behenate (AgBe) was used to calibrate scattering patterns.[38] Scattering data were reduced using the Nika package for Igor Pro[39] and plotted against the momentum transfer vector $q = (4\pi/\lambda) \sin \theta$.

RESULTS AND DISCUSSION

A P3EHT-*b*-PMA block copolymer was leveraged to study the detailed coupling between P3EHT crystallization and diblock copolymer domain structure as a function of thermal history. Furthermore, blends of P3EHT-*b*-PMA with PMA and P3EHT homopolymer probe the impact of PMA chain stretching and

DOI: 10.1021/acs.macromol.7b01616
Macromolecules 2017, 50, 8097−8105

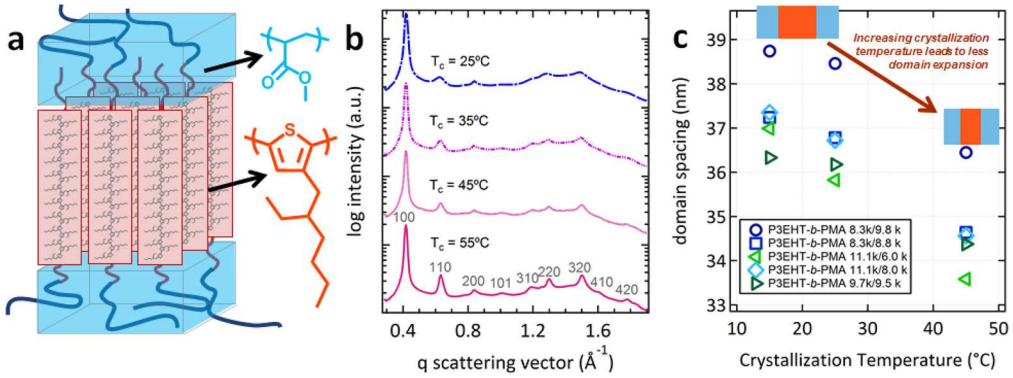

Figure 1. (a) Cartoon of crystalline P3EHT-*b*-PMA diblock copolymers containing rubbery poly(methyl acrylate) (PMA) and conjugated poly(3-(2′-ethyl)hexylthiophene) (P3EHT) components with P3EHT chains perpendicular to the domain interfaces. (b) The most compact final structure is also the structure with the highest quality crystallites via WAXS, similar to as seen in ref 26. (c) P3EHT-*b*-PMA diblock copolymers display the most expansion upon crystallization at lower temperatures measured via SAXS. Note that while these samples all demonstrated expanded domains at low T_c, the precise molecular weight dependent domain size scaling was variable; this is attributed to slight differences in molecular weight dispersity between samples.

P3EHT decoupling respectively on structure formation. While previous work has identified the P3EHT preference for extended chain crystals as critical for achieving crystallinity in confinement and driving the final domain structure, this study examines the detailed interactions moderating this structure.[26] The goal is to develop a model for how the constituent forces interact to control the resulting crystallinity and domain structure. In particular, temperature-dependent driving factors are expected to include changes in crystalline perfection, stretching of the coupled amorphous block induced by crystallization, and temperature-dependent chain diffusion and nucleation effects. Therefore, the roles of temperature in moderating these interactions are examined by tracking the domain structure as a function of crystallization temperature and as a detailed function of temperature during melting. Investigating the thermal responsive behavior of P3EHT-*b*-PMA domains reveals that, surprisingly, the final domain size is largest at large degrees of undercooling; higher crystallization temperatures result in more compact domains. Correlating these shifts to changes in the crystallinity as measured by DSC and WAXS challenges some of the assumed mechanisms of how improvements in order proceed in confinement, while clarifying the mechanism of melt-recrystallization. In particular, this work suggests that the primary changes in domain structure with thermal processing are connected to crystallization processes. Furthermore, over the regimes studied here, PMA chain stretching upon crystallization does not appear to be capable of inducing P3EHT chain folding according to a classical model, reinforcing the conclusion that extended chain crystallization is a key driver of structure.

Thermal History Impacts the Final Crystallization-Templated Domain Structure in Lamellar P3EHT-*b*-PMA. In developing block copolymers with confined conjugated polymer crystallization, it is important to understand the interactions between domain structure and crystallization. Importantly, many of the relevant forces and dynamics at play are temperature-dependent. Notably, chain diffusion kinetics improve as a function of temperature while nucleation processes become less favored with increasing temperature. Furthermore, the penalty of stretching PMA chains also increases as a function of temperature. Here, crystallinity is particularly highly coupled to the PMA chain stretching due to the observed orientation of P3EHT chains perpendicular to the P3EHT-*b*-PMA interface (Figure 1a); in principle, an equilibrium degree of chain folding in crystallites could be coupled to the degree of PMA chain stretching. In this work, the P3EHT-*b*-PMA system is an excellent system to study the roles of these highly coupled interactions due to the deformability of the rubbery PMA. While increasing crystallization temperatures leads to improved crystalline perfection (Figure 1b), domain size is not expected to change. This expectation rested on prior work on the diblock copolymer and homopolymer, which indicated that improvements in crystallinity with isothermal crystallization temperature lay mainly in the π-stacking direction.[26,27] If there were any change to be seen, an increase in domain size was expected with crystallization temperature due to more extended chains. Increased crystallization temperatures and improved crystalline perfection are often assumed to correspond to increasing degrees of chain extension by analogy to the well-understood processes of lamellar thickening in traditional flexible polymers.[30,31,40−45] Here, to probe these relationships, the domain structure across a family of diblock copolymers was measured as a function of isothermal crystallization temperature. The measurements definitively found that the final structure is indeed significantly moderated by the isothermal crystallization temperature—samples showed a variation in final structure size of as much as 10%. Across a range of molecular weights, and P3EHT volume fractions, lamellar diblocks displayed a common temperature-dependent response that is determined purely by a combination of the crystallization conditions and thermal history across this family of lamellar samples (Figure 1c). Surprisingly, however, the materials show the opposite trend to the expected one: the largest domains, and thus greatest degree of expansion, are observed at low crystallization temperatures, while the least is observed at high temperatures. This observation directly challenged assumptions of several of the fundamental processes and crystallite structuring occurring in these materials.

Several possibilities present themselves to explain this unexpected behavior. First, given that polymers become less dense with increasing temperature, the shrinking domains with increasing crystallization temperature cannot be explained by density-based arguments. Notably, P3EHT crystallization to form fully extended chains imposes a stretching penalty upon the coupled PMA block that increases as a function of

DOI: 10.1021/acs.macromol.7b01616
Macromolecules 2017, 50, 8097−8105

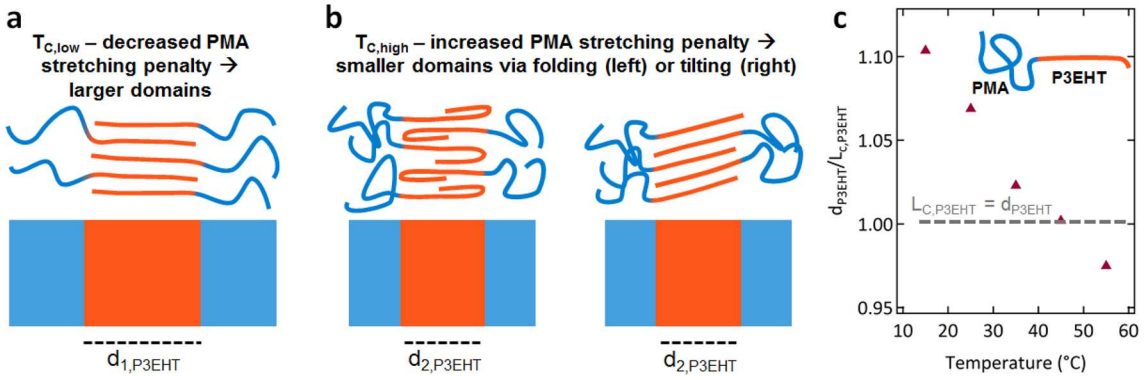

Figure 2. (a) Fully extended P3EHT chains induce a stretching penalty in coupled PMA chains, which is decreased at lower temperatures and could allow for larger domains. (b) As this penalty increases with temperature, it could induce folding (left) or tilting (right) in P3EHT chains, causing smaller overall domain size. (c) P3EHT domain size (from P3EHT-*b*-PMA 11.1K/6.0K) as a function of T_c is inconsistent with a model of integer chain folding. At low T_c, P3EHT domain sizes are ~10% larger than the P3EHT contour length.

temperature (Figure 2a).[33,34] The system can relieve this stretching penalty by either changing the orientation of crystallites relative to the interface or inducing folding within the P3EHT chain. Both of these responses create new energetic penalties as P3EHT chains will have to bend near the interface for a change in orientation, or along the chain length for folding, which are significant bending penalties within conjugated polymers. If crystallites tilt or reorient with chains parallel to domains as a function of temperature, this would effectively increase the area per chain at each interface, therefore reducing the penalty of stretching the amorphous PMA block (Figure 2b). However, our previous work examined the relative orientation of crystallites confined within lamellar diblock copolymers via SAXS/WAXS of aligned lamellae both as a function of T_c and during the melting process.[26] Regardless of the conditions, the orientation found is constant and is only consistent with crystalline P3EHT chains oriented perpendicular to the domain interfaces. Thus, the observed decreased domain spacing with increased T_c cannot be attributed to a balance between chain orientation and chain stretching penalties.

Alternatively, with increasing temperature, a chain-stretching penalty could induce folding of the associated crystallizable block (Figure 2b). To study this, a single sample (P3EHT-*b*-PMA 11.1k/6.0k) was examined in depth for the rest of the work. First, the normalized P3EHT domain size (relative to the P3EHT contour length) is found as a function of crystallization temperature (Figure 2c) using the constituent volume fractions. These results show that as the crystallization temperature increases, the P3EHT domain size (normalized to the M_n P3EHT contour length) decreases roughly linearly from 1.10 to slightly less than 1.00. These results emphasize that as the crystallization temperature increases, the P3EHT certainly does not chain fold by a traditional model. By a traditional model, we would expect a series of normalized P3EHT domain size of $d_{P3EHT}/L_{c,P3EHT}$ = 1.0, 0.5, 0.33, 0.25, etc., corresponding to 0, 1, 2, 3, etc., folds per chain with increasing domain temperature. Thus, if P3EHT is folding in confinement, it must instead be associated with only partial folding or folding only near the edges of P3EHT domains (as depicted in Figure 2b). Furthermore, the fact that at low temperatures the P3EHT domain size is considerably longer than the P3EHT contour length indicates that chains may not be fully interdigitated (as opposed to merely fully extended). At high T_c, the d_{P3EHT} is slightly larger than the (M_n-based) contour length of the P3EHT. Potentially, this could reflect local chain folding at the edges of crystallites; alternatively, this could be an effect from the P3EHT block's small but finite dispersity. Additional studies leveraged PMA and P3EHT homopolymers to selectively swell diblock microdomains. Unlike studies of hydrogenated polynorbornene crystallization in diblock copolymers where the amorphous block has a significant impact on the hydrogenated polynorbornene structure,[22] PMA chain-stretching penalties are not found to have a significant effect on P3EHT crystallinity or structure (Supporting Information Table 1 and Figures 2–5).

Domain and Thermal Transitions Are Highly Coupled on Melting. In crystalline homopolymers, polymer crystals cannot achieve an equilibrium structure; however, in principle they can form equilibrium block copolymer structures by achieving an equilibrium degree of chain folding.[22,33,34] However, this does not necessarily mean that the resulting structure will actually be in equilibrium. In particular, polymer crystallization is a highly hierarchical process that is also dependent upon nucleation and chain diffusion effects to achieve crystallinity; ultimately, this can result in secondary nucleation and other effects. To study the details of how P3EHT crystallization is coupled to the resulting domain structure, and to help deconvolute the relevant forces, a detailed investigation of the relationship between domain structure and crystallinity upon melting as a function of crystallization temperature (T_c = 25, 35, 45, and 55 °C) was performed, again focusing on the highlighted sample P3EHT-*b*-PMA 11.1k/6.0k. The domain size of the P3EHT-*b*-PMA structure was measured as a function of increasing temperature with high-temperature resolution in-situ SAXS (Supporting Information Figure 1). Melting clearly falls into three regimes, identifiable via shifts in *d*-spacing as identified by SAXS (Figure 3a); the onsets of these shifts correlate well with the onsets of melting peaks identified from differential scanning calorimetry (Figure 3b).

The first, broad low-temperature regime results in a large impact on domain structure, especially in diblock copolymers crystallized at low temperatures. Interestingly, upon tracking the domain spacing through this transition using SAXS, the materials display a very broad, slow change spread over a wide temperature window. Notably, the onset of the initial domain shrinkage by SAXS agrees well with the onset of this initial peak as melted by DSC. Peaks as measured by DSC show slightly earlier onsets and extend over a smaller temperature window

DOI: 10.1021/acs.macromol.7b01616
Macromolecules 2017, 50, 8097–8105

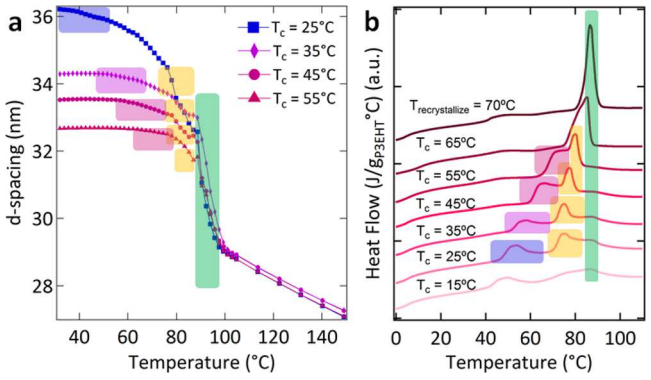

Figure 3. Domain spacing of P3EHT-*b*-PMA 11.1k/6.0k during heating and correlation of domain spacing changes to thermal transitions by DSC. (a) Onset of initial domain shrinkage during heating as well as final melting show excellent agreement with (b) initial and final features by DSC.

than the transitions by SAXS, which is likely an impact of the significantly faster scan rates in the DSC. For low-temperature crystallization, this initial relaxation corresponds to several nanometers of the total difference in domain spacing observed as a function of temperature; for high-temperature crystallized samples, it is merely on the order of half a nanometer. This significantly informs our model of the internal structure of the crystallites within the domains and their formation as a function of temperature. This low-temperature feature must correspond to an ordered region at the edges of the domains; across this low-temperature peak, these regions disorder and the parts of chains participating in it relax, resulting in a net shrinkage of the domains (Figure 4). At low T_c, a much larger shrinkage is observed over these low-temperature regions. This implies that low T_c causes a significantly larger amount of P3EHT to participate in these excluded regions. For T_c of 45 °C and greater, these features clearly begin to overlap; the regions highlighted in Figure 3 are intended as a guide to the eye.

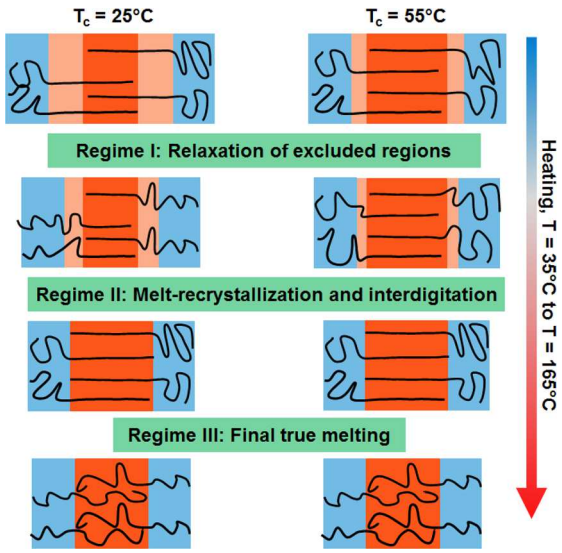

Figure 4. Cartoon of suggested relaxation and melting mechanism across the three regimes. Green labels correspond to transitions between figures. The initial state (top of figure) depends on T_c, which then influences the melting behavior until reaching a common domain and crystalline conformation at the beginning of regime III.

Correspondingly, with increasing T_c, this transition has an increasingly minimal impact on domain structure, implying that most of each chain is included in the central crystallites with higher T_c.

In order to elucidate the nature of the low-temperature peak, as well as to find improved methods for developing highly perfect crystallites, a P3EHT-*b*-PMA that was initially crystallized at 25 °C was subsequently annealed overnight at 70 °C. This reveals that (1) the material does not melt-recrystallize on the time scales of the DSC scan as it shows only a single peak on melting (Figure 3b) and that (2) postprocessing annealing can achieve higher degrees of perfection than manipulating the confined crystallites by varying the degree of undercooling alone. This behavior is similar to what we previously observed in P3EHT confined in cylindrical microdomains.[28] Furthermore, despite aging this sample at room temperature for 2 days after annealing at 70 °C prior to running the DSC, the broad low-temperature peak observed at temperatures just below the melt-recrystallization peak has vanished; only a weak feature at ∼40 °C remains, implying that negligible material remains participating in this excluded region. It is hypothesized that this excluded region is analogous to the rigid amorphous fraction observed in the analogous homopolymers.[46] The low-melting feature peaks observed here are large relative to those in the homopolymer but are not associated with a loss in crystalline scattering intensity;[26] it is hypothesized that here the tethering to the block copolymer interface and relative mobility of the PMA enhances the magnitude of material that participates in a rigid amorphous fraction relative to the homopolymer. The calculated crystallinity w_C of the narrow, unimodal melting peak from the sample annealed at 70 °C is ∼72%, using $w_C = \Delta H_m/\Delta H_m^\circ$.[27] Notably, this is comparable to the crystallinities of P3EHT homopolymer at similar molecular weights.[27] For most samples, crystallinities are not calculated due to significant uncertainties in the relative crystallite surface energies and size/shape in confinement, uncertainties in which parts of the DSC trace (with melt-recrystallization) uniquely belong to the initial crystallinity of the sample, and challenges with accurate baselining of extremely broad, multimodal melting peaks.

Interestingly, the origin of these excluded regions may be related to the balance between diffusion-limited and nucleation-limited crystallization. The P3EHT T_g is weak and challenging to directly observe directly via DSC but occurs at ∼10 °C. Thus, all crystallizations were performed above P3EHT's T_g (and indeed, the slow crystallization dynamics of P3EHT homopolymer allows a sticky, rubbery solid to be observed at 15 °C and higher before crystals form). However, chain dynamics are still temperature dependent, and recent work examining isothermal crystallization kinetics of P3EHT homopolymer has found that below 65 °C crystallization is limited by diffusion (i.e., P3EHT readily forms many nuclei, but slow chain diffusion makes the growth of crystallites challenging).[32] If indeed this is also the limitation in diblock copolymers, nucleation may create crystallites at the centers of domains that do not optimally interdigitate chains; additional growth and chain extension result in significant material excluded from the central crystallites. It is helpful to consider the steps required for perfect, fully extended crystallites to form directly from the melt—first, each crystal nucleus must initially form from the centers of two perfectly aligned polymer chains. Statistically, this scenario is unlikely. Thus, in the more probable scenario where a nucleus is formed from parts of the chains statistically closer to the ends of chains (farther from

DOI: 10.1021/acs.macromol.7b01616
Macromolecules 2017, 50, 8097−8105

the domain boundaries), the polymer will grow a crystallite from this site. Ultimately, at the edges of the domains, chains will no longer be fully interdigitated due to density restrictions and cannot participate in the crystallite. The T_c-dependent variability in exclusion is attributed to decreasing diffusion limitations on crystallization with higher temperature; over the examined range, diffusion limitations are expected to dominate over nucleation limitations.[32] Further, this model by which parts of chains are excluded from the center of the crystallite as a function of temperature is a satisfactory explanation for the observation that the measured P3EHT domain sizes are actually slightly more than the M_n-based P3EHT contour length for large degrees of undercooling (Figure 2c). Notably, this mechanism does not result in an equilibrium degree of exclusion for a given crystallization temperature.

Furthermore, the second melting regime provides additional insight into the melt-recrystallization mechanism in these materials. From domain spacing as a function of melting as tracked by SAXS, the transition from the first regime to the second is identified as the inflection point in curvature as a function of temperature (Figure 3a). It is important to note that the rate of temperature change in the SAXS (2 °C temperature resolution with 5 min sample equilibration times at each step) was very slow relative to the DSC (10 °C/min). Upon the onset of the second melting peak/second melting regime, samples showed a sudden decrease in domain spacing. The onset of this second melting regime—measured both by DSC and by the change in curvature of the SAXS domain melting—shifts to higher temperatures with T_c (Figure 3a,c; yellow). The SAXS measurements track the response of the coupled domain and crystallite structure with heating across this entire second regime, showing that eventually the domain size becomes nearly constant. Interestingly, the domain structures begin to converge at the end of the second melt-recrystallization regime. However, these measurements are surprising in several respects. First, while these are consistent with the initial degree of crystallite perfection being manipulated by T_c, it was surprising to find that the domain size apparently shrinks across melt-recrystallization. Importantly, we previously found that while order along the alkyl chain stacking direction did not change significantly during melt-recrystallization, significant improvements in order along the π-stacking direction were observed.[27] Furthermore, we found that the evidence did not support a model describing additional chain extension with improvements in crystallinity.[27] However, the further decrease in domain size during melting which is simultaneous with an improvement in crystalline order was surprising, as we did not expect to observe chain-folding during melt-recrystallization. This model is, however, consistent with this regime overcoming diffusion limitations and permitting local melting followed by allowing the previously excluded chain sections to interdigitate and recrystallize into a single population of highly perfect crystals (Figure 4). This model does result in more of the material along the length of the chain participating in the primary crystallite after melt-recrystallization, although it is not due to a change in the degree of chain folding. Importantly, identifying these changes in crystallite structure as a function of temperature—and attributing the different regimes to the component processes—would be extremely challenging in the homopolymer via standard techniques. That we can discern these processes in our system demonstrates the utility of manipulating diblock copolymer morphologies to investigate the constituent processes within conjugated diblock copolymer materials. However, further studies would be necessary to definitively show that these detailed processes of melt-recrystallization associated with interdigitation are not unique to the diblock and also occur in the homopolymer.

Finally, the last melting regime corresponds to the equilibrium melting of the crystallite in the diblock copolymer. The convergence of the final melting temperature is difficult to probe via DSC alone because at the faster melting rates diffusion limitations prevent some of the melt-recrystallization process. However, by slow melting, domain structure as measured via SAXS clearly shows that all samples finally melt—corresponding to a significant loss of extension—at the same temperature and nearly the same domain size (Figure 3a,b; green). These measurements provide additional support that these materials initially form imperfectly crystalline materials which then are improved via the melt-recrystallization process (Figure 4); furthermore, it emphasizes that the final melting is independent of thermal history and may correspond to an equilibrium-controlled temperature and domain size.

This study of the coupling between crystallite and domain structure reveals a number of key ideas. First, by studying this detailed coupling, this work has been able to elucidate a more intricate mechanism for how material is excluded from the primary crystallites during initial crystallization to form ordered regions; further, it shows how after melting of these adjacent excluded regions, this material is incorporated into the primary crystallites during the melt-recrystallization process, leading to an apparent shrinkage of the domains as interdigitation occurs. Observing this coupling is only possible due to this system design with a rubbery matrix that allows deformation in response to P3EHT crystallization. Further, it illustrates an approach to achieve highly crystalline conjugated materials in confinement and demonstrates that clearly understanding the crystallization dynamics—in particular, diffusion and nucleation limitations—are helpful during system design and processing. Finally, it is important to emphasize that the crystallization as a function of T_c observed here is clearly a diffusion-limited, highly nonequilibrium effect. Not only is it clear the observed perturbations of the lamellar structure is a result of both primary crystallization and secondary aging processes, which are intrinsically nonequilibrium, but also is clearly impacted by diffusion-controlled kinetics during crystallization. Furthermore, the diblock copolymer structure is clearly path dependent; a structure will not return to a given domain structure without melting and repeating isothermal crystallization. For example, a material that is crystallized at 25 °C, allowed to melt-recrystallize at 70 °C, and then returned to 25 °C will maintain the domain and crystallite structure of the recrystallized material, emphasizing that this is the more stable state.

■ CONCLUSIONS

Here, the relationships between diblock copolymer structure, crystallization, and thermal processing are investigated. The P3EHT-*b*-PMA system is an ideal model system with which to investigate this coupling due to the deformable nature of the PMA block; the tethering between P3EHT and PMA chains at the interface means that changes in P3EHT crystallite packing also directly impact the PMA structure. Furthermore, changes in the P3EHT crystalline structure are manifested as changes in the overall domain structure, allowing the overall diblock copolymer to behave as a highly sensitive probe to changes along the chain direction of the crystalline structure.

DOI: 10.1021/acs.macromol.7b01616
Macromolecules 2017, 50, 8097−8105

Surprisingly, this work finds that the overall domain size (and thus the along-chain crystallite dimensions) are inversely proportional to temperature; higher T_c results in more compact domains. This result directly contradicts previous assumptions that in conjugated polymers improvements in crystallite order/perfection are directly comparable to the lamellar thickening processes observed in flexible crystalline polymers, where with increasing isothermal crystallization temperature (or over the course of a melt-recrystallization process) chains become less folded and more extended. Here, by tracking the P3EHT domain size as a function of processing conditions, we found that chain folding that follows an integer number of folds definitively does not occur; local folding near the edges of domains remains a possibility.

By studying the detailed melting behavior of these materials via differential scanning calorimetry, we find three distinct melting regimes from which we suggest a model of crystallinity in confinement. We suggest that regions are excluded from the primary crystallite as a function of crystallization temperature; the first melting regime corresponds to relaxation of excluded components of chains; the second (melt-recrystallization) regime corresponds to interdigitation and incorporation of these chains within the main crystallite. This melt-recrystallization enables simultaneous improvements in order along the π-stacking directions. The final melting regimes corresponds to melting of these crystallites which, after melt-recrystallization, are structurally independent of their prior thermal history. This work demonstrates that leveraging a block copolymer containing conjugated components is a useful system for investigating the structural details of crystallinity. Finally, this work suggests that unique crystallization processes associated with conjugated polymers can result in unusual temperature-dependent behavior and suggests processing rules for achieving highly crystalline materials in confinement.

■ ASSOCIATED CONTENT

Supporting Information

The Supporting Information is available free of charge on the ACS Publications website at DOI: 10.1021/acs.macromol.7b01616.

Figures 1−5 and Table 1 (PDF)

■ AUTHOR INFORMATION

Corresponding Author

*E-mail segalman@engineering.ucsb.edu (R.A.S.).

ORCID

Rachel A. Segalman: 0000-0002-4292-5103

Notes

The authors declare no competing financial interest.

■ ACKNOWLEDGMENTS

We gratefully acknowledge support from the NSF-DMR Polymers Program through Grant 1608297. This work acknowledges user facilities at both the Advanced Light Source and the Stanford Synchrotron Radiation Lightsource, supported by the Director, Office of Science, Office of Basic Energy Sciences, of the U.S. Department of Energy under Contracts DE-AC02-05CH11231 and DE-AC02-76SF00515. We also gratefully acknowledge use of the UCSB MRL Shared Experimental Facilities supported by the MRSEC Program of the NSF under Award DMR 1121053; a member of the NSF-funded Materials Research Facilities Network. We also thank Rachel Behrens for support in the MRL polymer characterization facility.

■ REFERENCES

(1) Salleo, A. Charge transport in polymeric transistors. *Mater. Today* **2007**, *10* (3), 38−45.

(2) Sirringhaus, H.; Tessler, N.; Friend, R. H. Integrated optoelectronic devices based on conjugated polymers. *Science* **1998**, *280* (5370), 1741−1744.

(3) Thompson, B. C.; Frechet, J. M. J. Organic photovoltaics - Polymer-fullerene composite solar cells. *Angew. Chem., Int. Ed.* **2008**, *47* (1), 58−77.

(4) Himmelberger, S.; Dacuna, J.; Rivnay, J.; Jimison, L. H.; McCarthy-Ward, T.; Heeney, M.; McCulloch, I.; Toney, M. F.; Salleo, A. Effects of Confinement on Microstructure and Charge Transport in High Performance Semicrystalline Polymer Semiconductors. *Adv. Funct. Mater.* **2013**, *23* (16), 2091−2098.

(5) Himmelberger, S.; Duong, D. T.; Northrup, J. E.; Rivnay, J.; Koch, F. P. V.; Beckingham, B. S.; Stingelin, N.; Segalman, R. A.; Mannsfeld, S. C. B.; Salleo, A. Role of Side-Chain Branching on Thin-Film Structure and Electronic Properties of Polythiophenes. *Adv. Funct. Mater.* **2015**, *25* (17), 2616−2624.

(6) Jimison, L. H.; Himmelberger, S.; Duong, D. T.; Rivnay, J.; Toney, M. F.; Salleo, A. Vertical Confinement and Interface Effects on the Microstructure and Charge Transport of P3HT Thin Films. *J. Polym. Sci., Part B: Polym. Phys.* **2013**, *51* (7), 611−620.

(7) Tseng, H. R.; Phan, H.; Luo, C.; Wang, M.; Perez, L. A.; Patel, S. N.; Ying, L.; Kramer, E. J.; Nguyen, T. Q.; Bazan, G. C.; Heeger, A. J. High-Mobility Field-Effect Transistors Fabricated with Macroscopic Aligned Semiconducting Polymers. *Adv. Mater.* **2014**, *26* (19), 2993−2998.

(8) Snyder, C. R.; Kline, R. J.; DeLongchamp, D. M.; Nieuwendaal, R. C.; Richter, L. J.; Heeney, M.; McCulloch, I. Classification of Semiconducting Polymeric Mesophases to Optimize Device Post-processing. *J. Polym. Sci., Part B: Polym. Phys.* **2015**, *53* (23), 1641−1653.

(9) Kline, R. J.; McGehee, M. D.; Kadnikova, E. N.; Liu, J. S.; Frechet, J. M. J.; Toney, M. F. Dependence of regioregular poly(3-hexylthiophene) film morphology and field-effect mobility on molecular weight. *Macromolecules* **2005**, *38* (8), 3312−3319.

(10) DeLongchamp, D. M.; Kline, R. J.; Jung, Y.; Lin, E. K.; Fischer, D. A.; Gundlach, D. J.; Cotts, S. K.; Moad, A. J.; Richter, L. J.; Toney, M. F.; Heeney, M.; McCulloch, I. Molecular basis of mesophase ordering in a thiophene-based copolymer. *Macromolecules* **2008**, *41* (15), 5709−5715.

(11) Kline, R. J.; McGehee, M. D. Morphology and Charge Transport in Conjugated Polymers. *J. Macromol. Sci., Polym. Rev.* **2006**, *46* (1), 27−45.

(12) Loo, Y. L.; Register, R. A.; Ryan, A. J. Modes of crystallization in block copolymer microdomains: Breakout, templated, and confined. *Macromolecules* **2002**, *35* (6), 2365−2374.

(13) Loo, Y. L.; Register, R. A.; Ryan, A. J. Polymer crystallization in 25-nm spheres. *Phys. Rev. Lett.* **2000**, *84* (18), 4120−4123.

(14) Iovu, M. C.; Jeffries-El, M.; Zhang, R.; Kowalewski, T.; Mccullough, R. D. Conducting block copolymer nanowires containing regioregular poly(3-hexylthiophene) and polystyrene. *J. Macromol. Sci., Part A: Pure Appl. Chem.* **2006**, *43* (12), 1991−2000.

(15) Iovu, M. C.; Zhang, R.; Cooper, J. R.; Smilgies, D. M.; Javier, A. E.; Sheina, E. E.; Kowalewski, T.; McCullough, R. D. Conducting block copolymers of regioregular poly(3-hexylthiophene) and poly(methacrylates): Electronic materials with variable conductivities and degrees of interfibrillar order. *Macromol. Rapid Commun.* **2007**, *28* (17), 1816−1824.

(16) Ho, V.; Boudouris, B. W.; Segalman, R. A. Tuning Polythiophene Crystallization through Systematic Side Chain Functionalization. *Macromolecules* **2010**, *43* (19), 7895−7899.

DOI: 10.1021/acs.macromol.7b01616
Macromolecules 2017, 50, 8097−8105

(17) Ho, V.; Boudouris, B. W.; McCulloch, B. L.; Shuttle, C. G.; Burkhardt, M.; Chabinyc, M. L.; Segalman, R. A. Poly(3-alkylthiophene) Diblock Copolymers with Ordered Microstructures and Continuous Semiconducting Pathways. *J. Am. Chem. Soc.* **2011**, *133* (24), 9270−9273.
(18) Sadler, D. M.; Keller, A. Neutron-Scattering of Solution-Grown Polymer Crystals - Molecular Dimensions Are Insensitive to Molecular-Weight. *Science* **1979**, *203* (4377), 263−265.
(19) Liu, J. H.; Arif, M.; Zou, J. H.; Khondaker, S. I.; Zhai, L. Controlling Poly(3-hexylthiophene) Crystal Dimension: Nanowhiskers and Nanoribbons. *Macromolecules* **2009**, *42* (24), 9390−9393.
(20) McCulloch, B.; Ho, V.; Hoarfrost, M.; Stanley, C.; Do, C.; Heller, W. T.; Segalman, R. A. Polymer Chain Shape of Poly(3-alkylthiophenes) in Solution Using Small-Angle Neutron Scattering. *Macromolecules* **2013**, *46* (5), 1899−1907.
(21) Mulhearn, W. D.; Register, R. A. Melt Miscibility in Diblock Copolymers Containing Polyethylene and Substituted Hydrogenated Polynorbornenes. *Macromolecules* **2017**, *50* (15), 5830−5838.
(22) Lee, L. B. W.; Register, R. A. Equilibrium control of crystal thickness and melting point through block copolymerization. *Macromolecules* **2004**, *37* (19), 7278−7284.
(23) Mollinger, S. A.; Salleo, A.; Spakowitz, A. J. Anomalous Charge Transport in Conjugated Polymers Reveals Underlying Mechanisms of Trapping and Percolation. *ACS Cent. Sci.* **2016**, *2* (12), 910−915.
(24) Noriega, R.; Rivnay, J.; Vandewal, K.; Koch, F. P. V.; Stingelin, N.; Smith, P.; Toney, M. F.; Salleo, A. A general relationship between disorder, aggregation and charge transport in conjugated polymers. *Nat. Mater.* **2013**, *12* (11), 1038−1044.
(25) Rivnay, J.; Noriega, R.; Kline, R. J.; Salleo, A.; Toney, M. F. Quantitative analysis of lattice disorder and crystallite size in organic semiconductor thin films. *Phys. Rev. B: Condens. Matter Mater. Phys.* **2011**, *84* (4), 045203.
(26) Davidson, E. C.; Beckingham, B. S.; Ho, V.; Segalman, R. A. Confined Crystallization in Lamellae Forming Poly(3-(2 ′-ethyl)-hexylthiophene) (P3EHT) Block Copolymers. *J. Polym. Sci., Part B: Polym. Phys.* **2016**, *54* (2), 205−215.
(27) Beckingham, B. S.; Ho, V.; Segalman, R. A. Melting Behavior of Poly(3-(2′-ethyl)hexylthiophene). *Macromolecules* **2014**, *47* (23), 8305−8310.
(28) Davidson, E. C.; Segalman, R. A. Confined Crystallization within Cylindrical P3EHT Block Copolymer Microdomains. *Macromolecules* **2017**, *50* (16), 6128−6136.
(29) Snyder, C. R.; Henry, J. S.; DeLongchamp, D. M. Effect of Regioregularity on the Semicrystalline Structure of Poly(3-hexylthiophene). *Macromolecules* **2011**, *44* (18), 7088−7091.
(30) Nieuwendaal, R. C.; Snyder, C. R.; DeLongchamp, D. M. Measuring Order in Regioregular Poly(3-hexylthiophene) with Solid-State C-13 CPMAS NMR. *ACS Macro Lett.* **2014**, *3* (2), 130−135.
(31) Snyder, C. R.; Nieuwendaal, R. C.; DeLongchamp, D. M.; Luscombe, C. K.; Sista, P.; Boyd, S. D. Quantifying Crystallinity in High Molar Mass Poly(3-hexylthiophene). *Macromolecules* **2014**, *47* (12), 3942−3950.
(32) Yu, L.; Davidson, E. C.; Sharma, A.; Andersson, M. R.; Segalman, R. A.; Müller, C. Isothermal Crystallization Kinetics and Time-Temperature-Transformation of the Conjugated Polymer: Poly(3-(2′-ethyl)hexylthiophene). *Chem. Mater.* **2017**, *29* (13), 5654−5662.
(33) Whitmore, M. D.; Noolandi, J. Theory of Crystallizable Block Copolymers. *Makromol. Chem., Macromol. Symp.* **1988**, *16*, 235−249.
(34) Douzinas, K. C.; Cohen, R. E.; Halasa, A. F. Evaluation of Domain Spacing Scaling Laws for Semicrystalline Diblock Copolymers. *Macromolecules* **1991**, *24* (15), 4457−4459.
(35) Chen, H. L.; Hsiao, S. C.; Lin, T. L.; Yamauchi, K.; Hasegawa, H.; Hashimoto, T. Microdomain-tailored crystallization kinetics of block copolymers. *Macromolecules* **2001**, *34* (4), 671−674.
(36) Zhu, L.; Chen, Y.; Zhang, A. Q.; Calhoun, B. H.; Chun, M. S.; Quirk, R. P.; Cheng, S. Z. D.; Hsiao, B. S.; Yeh, F. J.; Hashimoto, T. Phase structures and morphologies determined by competitions among self-organization, crystallization, and vitrification in a disordered poly(ethylene oxide)-b-polystyrene diblock copolymer. *Phys. Rev. B: Condens. Matter Mater. Phys.* **1999**, *60* (14), 10022−10031.
(37) Olsen, B. D.; Segalman, R. A. Structure and thermodynamics of weakly segregated rod-coil block copolymers. *Macromolecules* **2005**, *38* (24), 10127−10137.
(38) Huang, T. C.; Toraya, H.; Blanton, T. N.; Wu, Y. X-Ray-Powder Diffraction Analysis of Silver Behenate, a Possible Low-Angle Diffraction Standard. *J. Appl. Crystallogr.* **1993**, *26*, 180−184.
(39) Ilavsky, J. Nika: software for two-dimensional data reduction. *J. Appl. Crystallogr.* **2012**, *45*, 324−328.
(40) Hoffman, J. D.; Lauritzen, J. I. Crystallization of Bulk Polymers with Chain Folding - Theory of Growth of Lamellar Spherulites. *J. Res. Natl. Bur. Stand., Sect. A* **1961**, *65A* (4), 297.
(41) Lauritzen, J. I.; Hoffman, J. D. Extension of Theory of Growth of Chain-Folded Polymer Crystals to Large Undercoolings. *J. Appl. Phys.* **1973**, *44* (10), 4340−4352.
(42) Hoffman, J. D.; Weeks, J. J. Melting Process and Equilibrium Melting Temperature of Polychlorotrifluoroethylene. *J. Res. Natl. Bur. Stand., Sect. A* **1962**, *66A* (1), 13.
(43) Hoffman, J. D.; Weeks, J. J. X-Ray Study of Isothermal Thickening of Lamellae in Bulk Polyethylene at Crystallization Temperature. *J. Chem. Phys.* **1965**, *42* (12), 4301.
(44) Koch, F. P. V.; Heeney, M.; Smith, P. Thermal and Structural Characteristics of Oligo(3-hexylthiophene)s (3HT)(n), n = 4−36. *J. Am. Chem. Soc.* **2013**, *135* (37), 13699−13709.
(45) Marsh, H. S.; Reid, O. G.; Barnes, G.; Heeney, M.; Stingelin, N.; Rumbles, G. Rumbles, G., Control of Polythiophene Film Microstructure and Charge Carrier Dynamics Through Crystallization Temperature. *J. Polym. Sci., Part B: Polym. Phys.* **2014**, *52* (10), 700−707.
(46) Beckingham, B. S.; Ho, V.; Segalman, R. A. Formation of a Rigid Amorphous Fraction in Poly(3-(2′-ethyl)hexylthiophene). *ACS Macro Lett.* **2014**, *3* (7), 684−688.

DOI: 10.1021/acs.macromol.7b01616
Macromolecules 2017, 50, 8097−8105